ISSN 0036-0295, Russian Metallurgy (Metally), Vol. 2021, No. 2, pp. 213–218. © Pleiades Publishing, Ltd., 2021.
Russian Text © The Author(s), 2020, published in Rasplavy, 2020, No. 6, pp. 589–598.

# Dissolution of $Al_2O_3$ in $KF–AlF_3$

**P. S. Pershin[a], *, A. V. Suzdaltsev[a], and Yu. P. Zaikov[a, b]**

[a] *Institute of High-Temperature Electrochemistry, Ural Branch, Russian Academy of Sciences, Yekaterinburg, Russia*

[b] *Ural Federal University, Yekaterinburg, Russia*

**e-mail: pspershin@ihte.uran.ru*

Received June 28, 2020; revised July 18, 2020; accepted July 24, 2020

**Abstract**—$KF–AlF_3–Al_2O_3$-based melts are promising media for the electrolytic production of aluminum in next-generation energy efficient cells. This work analyzes the dissolution of $Al_2O_3$ in the $KF–AlF_3$ melt with a mole ratio $[KF]/[AlF_3] = 1.5$ mol/mol at 785°C using cyclic voltammetry and the carbothermic reduction of melt samples using a LECO analyzer. The measurements are performed by a cell consisting of a carbon glass working electrode, a $CO/CO_2$ gas reference electrode, and a graphite counter electrode. During measurements, the current response peak on voltammograms is recorded as a function of the potential scan rate, the dissolution time of the next alumina sample, and the alumina content in the melt. The current response peak is shown to linearly depend on the $Al_2O_3$ content in the melt, and the oxide dissolution rate is from $2.4 \times 10^{-3}$ to $5.45 \times 10^{-5}$ mol/s as a function of the oxide content in the melt. The obtained results demonstrate general possibility of operating nondestructive control of the alumina ($Al_2O_3$) content during the electrolysis of $KF–AlF_3–Al_2O_3$–based melts. It includes the recording of a current response peak in current–voltage curves and the determination of the current alumina content in a melt using the obtained empirical dependence.

**Keywords:** electrolysis of aluminum, alumina, $KF–AlF_3–Al_2O_3$, dissolution, dissolution rate, voltammetry

**DOI:** 10.1134/S0036029521020191

## INTRODUCTION

The main method of aluminum production for more than one hundred years is the electrolysis of a cryolite–alumina melt. Herewith, the alumina content in an electrolyte is one of the key electrolysis parameters, since it significantly influences the physicochemical properties of a cryolite–alumina melt [1].

At present, alumina is added to an electrolysis bath during the process by means of an alumina point feeder (APF), the main control variable of which is the bath voltage determined among others by the alumina content (both dissolved and undissolved) in a cryolite–alumina melt [1–3]. A drawback of this adjustment is that an increase in the bath voltage can be caused by both a decrease in the alumina content in the melt and its increase above 3–4 wt %. As a consequence, the voltage adjustment of feeding the bath with alumina becomes inefficient, and an incorrect APF operation mode results in the degradation of the process parameters (decrease in the anode current efficiency, increase in the voltage, increase in the specific energy consumption, etc.) and the reduction of the bath operation time. In this regard, the development of a method for operating control of the alumina content in cells is an important and challenging problem, including the development of complex mathematical models of alumina dissolution and distribution.

Since new efficient technologies and electrolysis cells for aluminum production are being actively developed [4–6], the study of alumina ($Al_2O_3$) dissolution in a cryolite–alumina melt and new low-melting electrolytes aiming at operating control of its content during electrolysis becomes even more important. From an analysis of available data, it follows that the alumina content can be determined most precisely and quickly by combination of the following two methods:

(i) the in-situ measurement of the property or parameter of the system in a cell, which correlates reliably and reasonably with the content of dissolved alumina in a melt;

(ii) physicochemical analysis of melt samples from a cell.

The solubility and dissolution kinetics of oxides in fluoride melts are analyzed using the following methods:

(a) potentiometry (emf of concentration cell) [2, 6–8],

(b) rotating disc electrode [9],

(c) voltammetry (anode current peak) [10–12],

(d) chronopotentiometry (transition time) [13, 14],

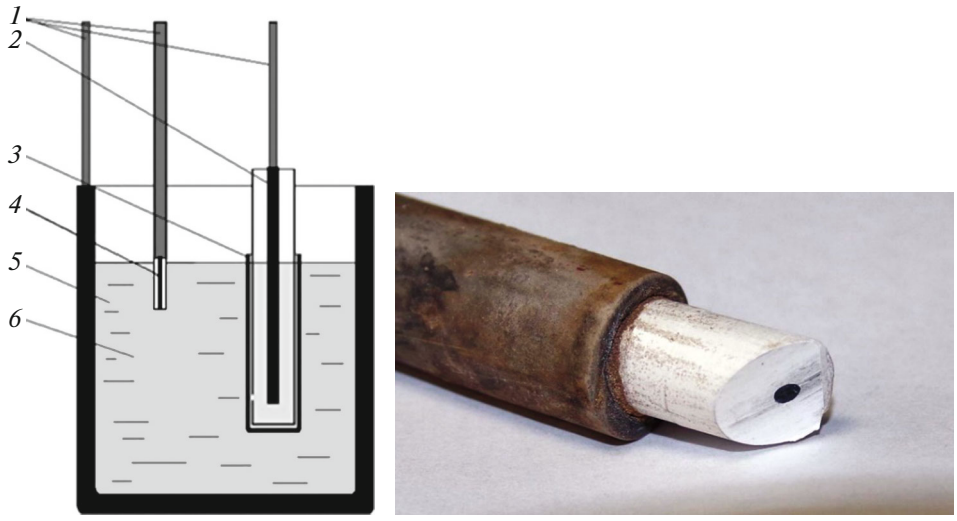


**Fig. 1.** Schematic of the experimental cell and photograph of the working electrode: (*1*) steel current leads, (*2*) $CO/CO_2$ gaseous electrode, (*3*) porous graphite crucible, (*4*) working end-face electrode (CG rod shielded with boron nitride), (*5*) melt to be studied, and (*6*) graphite crucible (counter electrode).

(e) thermal analysis (liquidus point) [3, 15],

(f) impedometry (electric conductivity of melt) [16, 17],

(g) stationary polarization (anode overvoltage) [18, 19],

(h) optical method (variation of melt structure) [20],

(i) visual method (existence of alumina suspension in melt) [8, 21, 22].

This work is aimed at studying certain regularities of the $Al_2O_3$ dissolution in the $KF–AlF_3$ melt by cyclic voltammetry and analyzing of the possibility of operating control of the alumina content in the melts under study.

## EXPERIMENTAL

The $Al_2O_3$ dissolution was studied in the $KF–AlF_3$ melt with the molar ratio $[KF]/[AlF_3] = 1.5$ mol/mol and various oxide contents in air at 785°C. The melt was prepared according to the procedure in [23] using individual salts, namely, reagent grade potassium fluoride KF and reagent grade aluminum fluoride $AlF_3$ (Vekton, Russia). Reagent grade aluminum oxide (Reakhim, Russia) was used as oxygen containing additive.

The measurements were carried out in a three-electrode electrochemical cell schematically illustrated in Fig. 1. Carbon glass (CG) rod *4* shielded with sintered boron nitride (Unikhim, Russia) and immersed into the melt was used as a working electrode. A graphite crucible with the melt was used as an auxiliary electrode. A $CO/CO_2$ gaseous electrode was used as reference electrode *2* located in a porous graphite crucible [24]. The working electrode was periodically taken from the melt for polishing and renewal of the surface.

Electrochemical measurements were made using a PGSTAT AutoLab 320N device and the NOVA 1.11 software (Metrohm, the Netherlands). Voltammograms were obtained at a potential scan rate from 1 to 20 V/s. The resistance voltage drop (IR) was compensated by the I-Interrupt procedure.

The furnace and melt temperatures were preset and controlled by means of Pt/Pt–Rh thermocouples, a Varta TP-703 thermal regulator, and a USB-TC01 thermocouple unit (National Instruments, United States).

To analyze the melt composition during measurements, melt samples 0.2–0.3 g in weight were taken using a nickel spoon. Prior to analysis, the samples were stored in a sealed dry box with an inert atmosphere. The alumina content in the samples was determined by carbothermic combustion with subsequent recording of absorption of infrared radiation in an exhaust gas flow using an OH 836 analyzer (LECO, United States). The elemental composition of the melts was determined by inductively coupled plasma atomic emission spectrometry using an iCAP 6300 Duo spectrometer (Thermo Scientific, United States).

## RESULTS AND DISCUSSION

### *Current–Voltage Measurements*

Figure 2 shows the voltammograms recorded for the $KF–AlF_3$ melt with 2.36 wt % $Al_2O_3$. When the potential is scanned toward the anode side, a peak is observed at 1.5–1.6 V; it is related to the oxidation of oxygen ions contained in electrically active oxide fluoride anion groups. The sharp current drop to 0.03–

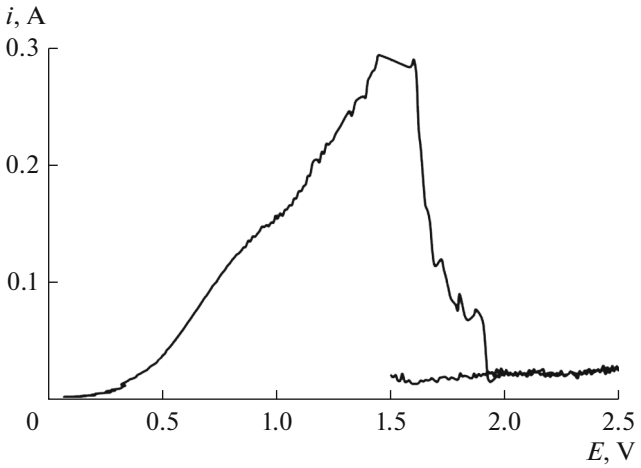


**Fig. 2.** Voltammogram recorded for molten KF–$AlF_3$ ([KF]/[$AlF_3$] = 1.5) with 2.36 wt % $Al_2O_3$ at 785°C and a scan rate of 1 V/s.

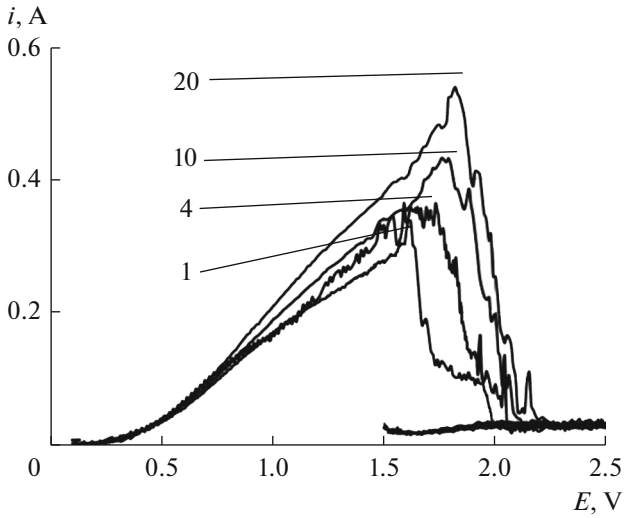


**Fig. 3.** Voltammograms recorded for molten KF–$AlF_3$ with 3.15 wt % $Al_2O_3$ at 785°C and a scan rate of 1–20 V/s.

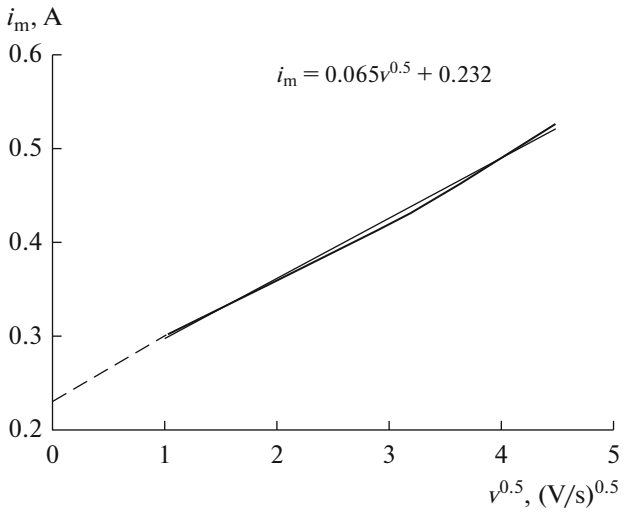


**Fig. 4.** Peak current as a function of the squared potential scan rate in molten KF–$AlF_3$ with 3.15 wt % $Al_2O_3$ at 785°C.

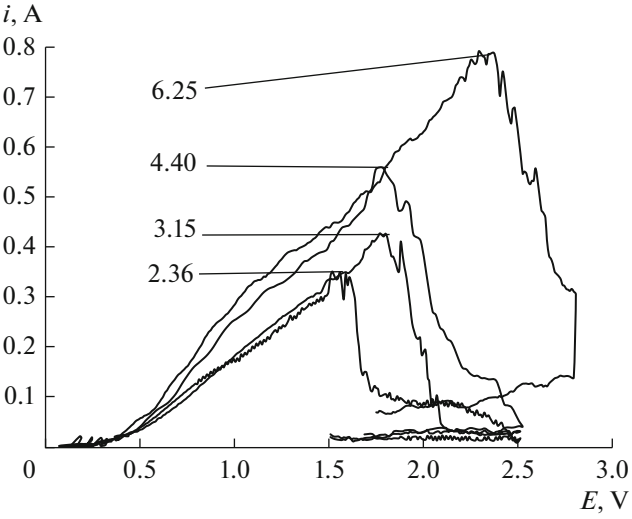


**Fig. 5.** Voltammograms recorded for molten KF–$AlF_3$ at 785°C and a scan rate of 1 V/s as a function of the $Al_2O_3$ content.

0.04 A upon further polarization is related to the depletion of near-anode layer of oxygen ions and start of the anode effect [10, 11]. Similar voltammograms were recorded for [11] upon studying the anode process kinetics on graphite in low-melting NaF–$AlF_3$–$Al_2O_3$ melts ([NaF]/[$AlF_3$] = 1.2 mol/mol).

Figure 3 shows the voltammograms recorded for the KF–$AlF_3$ melt with 3.15 wt % $Al_2O_3$ as a function of the potential scan rate. The peaks in the voltammograms are seen to form at a potential scan rate of 1 V/s, and an increase in the potential scan rate results in an increase in the current response peak. The peak current as a function of the squared scan rate is linear (Fig. 4); herewith, its extrapolation does not intersect the origin of coordinates, which indicates a mixed character of the obstacles to the process.

### *Estimation of the $Al_2O_3$ Content*

Figure 5 shows the voltammograms recorded for the KF–$AlF_3$ melt with various $Al_2O_3$ contents, and Fig. 6 shows the current response peak as an empirical function of the $Al_2O_3$ content in the melt. The response peak is seen to increase linearly with the $Al_2O_3$ content in the melt. Therefore, the obtained empirical dependence can be used for operating nondestructive control of the $Al_2O_3$ content during the electrolysis of the KF–$AlF_3$–$Al_2O_3$ melts, including recording of a current response peak in the current–

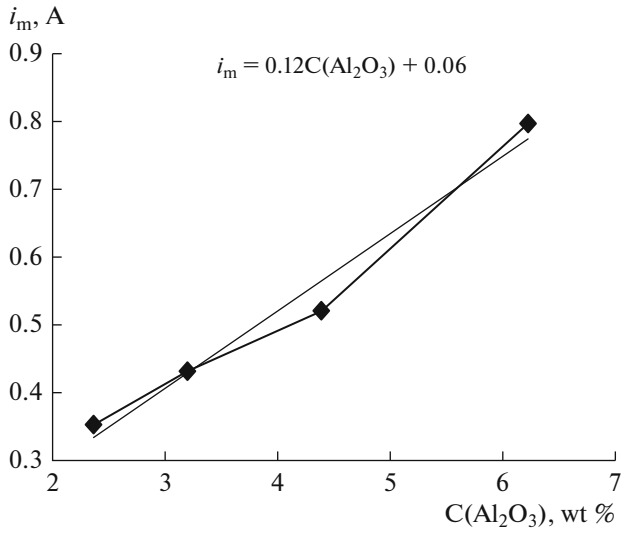


**Fig. 6.** $Al_2O_3$ content in molten KF–$AlF_3$–$Al_2O_3$ ([KF]/[$AlF_3$] = 1.5) at 785°C.

voltage curve and the determination of the current $Al_2O_3$ content in the melt using a preliminary obtained empirical dependence.

During this control, it is possible to determine the dynamics of changes in the $Al_2O_3$ content and, hence, the correctness of operation of $Al_2O_3$ automatic feeding to a cell.

### *Estimation of the $Al_2O_3$ Dissolution Rate*

In addition to the determination of the current $Al_2O_3$ content, the applicability of the method was tested by estimating the $Al_2O_3$ dissolution rate in the KF–$AlF_3$ melt ([KF]/[$AlF_3$] = 1.5 mol/mol) with various $Al_2O_3$ contents at 785°C. After feeding the next oxide portion into the melt, current–voltage curves were recorded in time.

Further measurements were carried out at a potential scan rate of 1 V/s. The first set of voltammograms was recorded immediately after feeding $Al_2O_3$ into the melt; then, one measurement every 30 s was made until the end of growth of the anode peak current. These measurements are exemplified in Fig. 7. It can be seen that the current response peak increases in time after feeding oxide, the current increase is maximal during the initial 0–5 s, and it then slows down. In this example, the current ceased to grow after 180–300 s, which indicates complete dissolution of a sample.

It should be mentioned that, upon visual observation, the dissolution of $Al_2O_3$ in the KF–$AlF_3$–$Al_2O_3$ melt at 785°C takes place much faster: after addition,

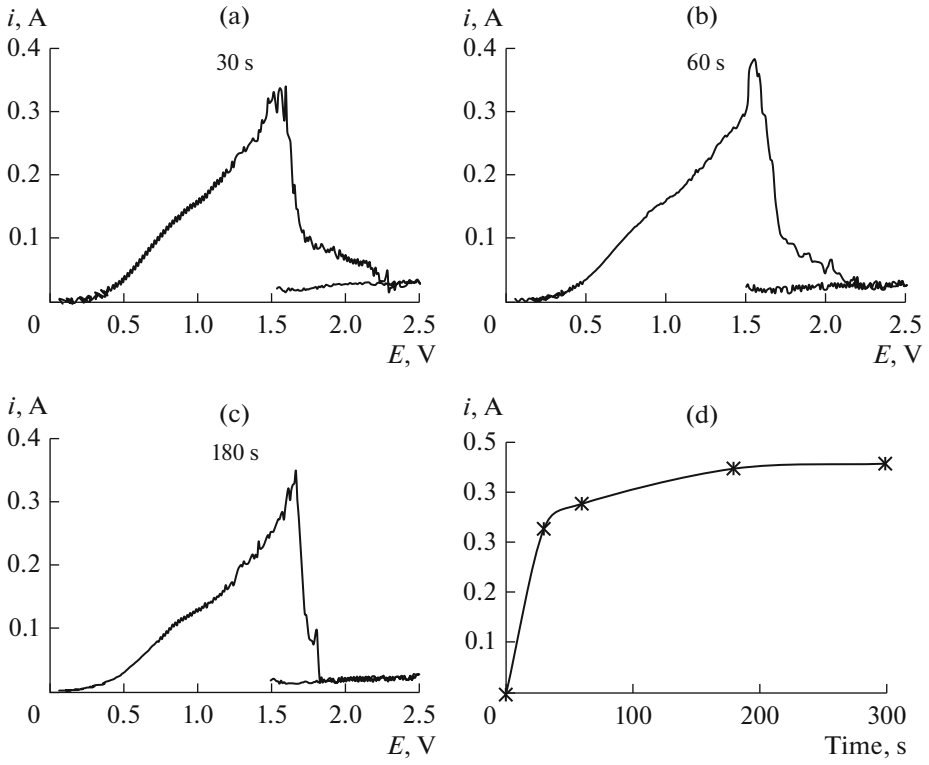


**Fig. 7.** Voltammograms recorded for molten KF–$AlF_3$ upon changes in the $Al_2O_3$ content in the melt from 2.36 to 3.15 wt % after (a) 30, (b) 60, and (c) 180 s. (d) Change in the current response peak in the voltammograms obtained on CG anode in molten KF–$AlF_3$ when the $Al_2O_3$ content in the melt changes from 2.36 to 3.15 wt % in time.

**Table 1.** Dissolution rates of alumina $Al_2O_3$ in molten $[KF]/[AlF_3]$ = 1.5 mol/mol at 785°C

| Change in $Al_2O_3$ in melt | | Dissolution rate, mol/s | |
|---|---|---|---|
| wt % | mol % | in initial 30 s | integrated |
| 2.36–3.15 | 1.61–2.16 | $2.4 \times 10^{-3}$ | – |
| 3.15–4.40 | 2.16–3.02 | $5.9 \times 10^{-4}$ | $5.45 \times 10^{-5}$ |
| 4.40–6.25 | 3.02–4.32 | $3.1 \times 10^{-4}$ | – |

an $Al_2O_3$ sample is on the melt surface for 1–5 s, and it then dissolves in the melt volume in 5–10 s.

However, the distribution of dissolved $Al_2O_3$ in the electrolyte volume and the diffusion of electrically active ions to the electrode surface take longer time, which was detected in recording of voltammograms. On the basis of the obtained data, we estimated the $Al_2O_3$ dissolution rates in the $KF–AlF_3$ melt with various initial $Al_2O_3$ contents at 785°C. The changes in the $Al_2O_3$ moles in the melt (according to LECO data) were divided by the sample dissolution time.

In general, it should be mentioned that the dissolution of $Al_2O_3$ in low-melting melts can be studied as a function of other experimental conditions using similar schemes.

## CONCLUSIONS

The dissolution of $Al_2O_3$ in the $KF–AlF_3$ melt with the mole ratio $[KF]/[AlF_3]$ = 1.5 mol/mol at 785°C was analyzed by cyclic voltammetry and carbothermic reduction of samples using LECO analyzer.

The current peak in the recorded voltammograms was shown to depend linearly on the $Al_2O_3$ content in the melt, and the alumina dissolution rate was estimated at $2.4 \times 10^{-3}$ to $5.45 \times 10^{-5}$ mol/s.

Using the current peak in the recorded voltammograms as a function of the $Al_2O_3$ content dissolved in the melt, we plotted a calibration curve. However, this dependence can only be applied for a specific melt composition, process temperature, and potential scan rate.

Analyzing the obtained results, we demonstrated the fundamental possibility of operating nondestructive control of the $Al_2O_3$ content during the electrolysis of $KF–AlF_3–Al_2O_3$-based melts. It includes recording of a current response peak on current–voltage curves and the determination of the current alumina content in the melt using the empirical dependence.

## ACKNOWLEDGMENTS

We are grateful to O.B. Pavlenko for the LECO analysis of samples.

## REFERENCES

1. Yu. V. Borisoglebskii, G. V. Galevskii, N. M. Kulagin, and M. Ya. Mintsis, *Metallurgy of Aluminum* (Nauka, Novosibirsk, 1999).
2. L. Bracamonte, K. Nilsen, Ch. Rosenkilde, and E. Sandes, "Alumina concentration measurements in cryolite melts," TMS: Light Metals, 600–607 (2020).
3. E. Skybakmoen, A. Solheim, and A. Sterten, Metall. Mater. Trans. B **27**, 81–86 (1997).
4. J. Yang, J. N. Hryn, B. R. Davis, A. Roy, G. K. Krumdick, J. A. Pomykala Jr., "New opportunities for aluminium electrolysis with metal anodes in a low temperature electrolyte system," TMS: Light Metals, 321–326 (2004).
5. A. Yu. Nikolaev, A. S. Yasinskii, A. V. Suzdaltsev, P. V. Polyakov, and Yu. P. Zaikov, "Electrolysis of aluminum in $KF–AlF_3–Al_2O_3$ melts and suspensions," Rasplavy, No. 3, 205–213 (2017).
6. A. S. Yasinskiy, A. V. Suzdaltsev, S. K. Padamata, P. V. Polyakov, and Yu. P. Zaikov, "Electrolysis of low–temperature suspensions: an update," TMS: Light Metals, 626–636 (2020).
7. N. V. Vasyunina, I. P. Vasyunina, Yu. G. Mikhalev, and A. M. Vinogradov, "Solubility and dissolution rate of alumina in acidic cryolite–alumina melts," Izv. Vyssh. Uchebn. Zaved., Tsvetn. Metall. **4**, 24–28 (2009).
8. A. V. Frolov, A. O. Gusev, Yu. P. Zaikov, A. P. Khramov, N. I. Shurov, O. Yu. Tkacheva, A. P. Apisarov, and V. A. Kovrov, "Modified alumina–cryolite bath with high electrical conductivity and dissolution rate of alumina," TMS: Light Metals, 571–576 (2007).
9. E. J. Frazer and J. Thonstad, Metall. Mater. Trans. B **41**, 543–548 (2010).
10. N. E. Richards, S. Rolseth, J. Thonstad, and R. G. Haverkamp, "Electrochemical analysis of alumina dissolved in cryolite melts," TMS: Light Metals, 391–404 (1995).
11. R. G. Haverkamp, S. Rolseth, J. Thonstad, and H. Gudbrandsen, "Voltammetry and electrode reactions in $AlF_3$-rich electrolyte," TMS: Light Metals, 481–486 (2001).
12. A. Yu. Nikolaev, O. B. Pavlenko, A. V. Suzdaltsev, and Yu. P. Zaikov, J. El. Chem. Soc. (2020) (in print).
13. R. K. Jain, H. C. Gaur, E. J. Frazer, and B. J. Welch, J. El. Analyt. Chem. **78**, 1–30 (1977).
14. V. N. Nekrasov, O. V. Limanovskaya, A. V. Suzdaltsev, Yu. P. Zaikov, and A. P. Khramov, "Carbon anode chronopotentiometry in $KF–AlF_3–Al_2O_3$ melts," Rasplavy, No. 2, 18–29 (2011).

15. A. E. Dedyukhin, A. P. Apisarov, O. Yu. Tkacheva, A. A. Redkin, Yu. P. Zaikov, A. V. Frolov, and A. O. Gusev, "The electrical conductivity of the molten system [(KF–$AlF_3$)–NaF]–$Al_2O_3$," Rasplavy, No. 2, 23–28 (2009).

16. A. A. Kataev, O. Yu. Tkacheva, I. D. Zakiryanova, A. A. Apisarov, A. E. Dedyukhin, and Yu.P. Zaikov, J. Mol. Liq. **231**, 149–153 (2017). https://doi.org/10.1016/j.molliq.2017.02.021

17. A. S. Yasinskiy, A. V. Suzdaltsev, P. V. Polyakov, S. K. Padamata, and O. V. Yushkova, Cer. Inter. B **46** (8), 11539–11548 (2020). https://doi.org/10.1016/j.ceramint.2020.01.180

18. V. A. Kovrov, A. P. Khramov, Yu. P. Zaikov, and N. I. Shurov, Rus. J. El. Chem. **43**, 909–919 (2007).

19. A. V. Suzdaltsev, V. N. Nekrasov, Yu. P. Zaikov, A. P. Khramov, and O. V. Limanovskaya, "Anodic polarization on glassy carbon in low-melting potassium cryolite–alumina melts," Rasplavy, No. 4, 41–51 (2009).

20. H.-M. Kan, N. Zhang, and X. Wang, J. Cent. South Univ. **19**, 897–902 (2012).

21. L. A. Isaeva, A. B. Braslavskii, and P. V. Polyakov, Izv. Vyssh. Uchebn. Zaved., Tsvetn. Metall. **6**, 35–41 (2009).

22. B. J. Welch and G. I. Kuschel, JOM **5**, 50–54 (2007).

23. A. Yu. Nikolaev, A. V. Suzdaltsev, and Yu. P. Zaikov, "A new method for the synthesis of Al–Sc master alloys in oxide–fluoride and fluoride melts," Rasplavy, No. 2, 155–165 (2020).

24. A. V. Suzdaltsev, A. P. Khramov, and Yu. P. Zaikov, "Carbon electrode for electrochemical studies in cryolite–alumina melts at 700–960°C," Electrokhimiya **48** (12), 1251–1263 (2012).

*Translated by I. Moshkin*